Particle acceleration at ultrarelativistic, perpendicular shock fronts

John G. Kirk, Brian Reville, Zhi-Qiu Huang
 Max-Planck-Institut für Kernphysik, Postfach 10 39 80, 69029 Heidelberg, Germany

7 December 2022

ABSTRACT

Using an eigenfunction expansion to solve the transport equation, complemented by Monte-Carlo simulations, we show that ultrarelativistic shocks can be effective particle accelerators even when they fail to produce large amplitude turbulence in the downstream plasma. This finding contradicts the widely held belief that a uniform downstream magnetic field perpendicular to the shock normal inhibits acceleration by the first order Fermi process. In the ultrarelativistic limit, we find a stationary power-law particle spectrum of index $s = 4.17$ for these shocks, close to that predicted for a strictly parallel shock.

Key words: radiation mechanisms: non-thermal — acceleration of particles — gamma rays: bursts

1 INTRODUCTION

Discovered in the late 1970s, the theory of diffusive shock acceleration has established itself as the primary mechanism discussed in connection with the acceleration of cosmic rays, and has also found many other applications. The generalisation of this mechanism to mildly relativistic shock fronts followed roughly a decade later, and, in the early 2000's, it was found that particles repeatedly crossing ultrarelativistic shocks can be accelerated into a power law spectrum of index $s = 4.23$ (for recent reviews, see Bell 2014; Sironi et al. 2015).

However, in contrast to the nonrelativistic case, an ultrarelativistic shock that overruns a region containing a uniform magnetic field is generically superluminal, in the sense that its speed, when projected onto a magnetic field line, exceeds that of light. At first sight, this poses a problem, since acceleration requires repeated crossings of the shock front, and a particle downstream of the shock cannot catch up with it by simply diffusing along a magnetic field line. Since cross-field diffusion is generally strongly suppressed, this suggests that the relativistic extension of the diffusive shock acceleration mechanism might be ineffective (Begelman & Kirk 1990).

This problem does not arise if the downstream field is effectively scrambled by strong fluctuations on the scale of a gyroradius (Achterberg et al. 2001). However, a mechanism for producing such fluctuations has so far not been identified. For the case of shock propagation into a weakly magnetized plasma, where the Weibel instability is thought responsible for the formation of the shock front, particle-in-cell simulations have shown that acceleration is facilitated by non-resonant scattering on the Weibel-induced filaments (e.g. Sironi & Spitkovsky 2009; Plotnikov et al. 2018; Vanthieghem et al. 2020). However, analytical considerations suggest that scattering exclusively mediated by such non-resonant interactions is not sufficient to provide the required cross-field transport in the downstream plasma above a critical particle energy (Lemoine & Pelletier 2010; Reville & Bell 2014; Huang et al. 2022). Furthermore, such short length-scale fluctuations are susceptible to damping in the hot downstream plasma, which further reduces the critical energy (Chang et al. 2008; Keshet et al. 2009; Sironi et al. 2013; Lemoine 2015)

In this paper, we re-assess these arguments by solving a simple model of a relativistic, perpendicular shock, thereby demonstrating quantitatively that particles are accelerated into a power-law distribution whose index lies very close to that predicted for the idealized, parallel shock case (Kirk et al. 2000). In our model, energetic particles are assumed to diffuse in angle, whilst being deflected by a uniform magnetic field that is *perpendicular* to the shock normal. We solve this model for the case in which transport upstream is scattering dominated, i. e., the particles there are *unmagnetized*, whereas particles are *magnetized* when downstream and follow essentially unscattered trajectories, gyrating about the regular, uniform magnetic field. Two complementary techniques are employed. First, we use a generalisation of the eigenfunction approach (Kirk et al. 2000) that takes into account the full, two-dimensional anisotropy imposed on the particle distribution, including the drift induced by the downstream magnetic field. This technique is applied in the ultrarelativistic limit of large shock Lorentz factor, $\Gamma_s \to \infty$, which enables the eigenfunctions to be found in closed form. The second method of solution is a Monte-Carlo simulation of many individual trajectories, using a code described more fully in a companion paper (Huang et al. 2023, henceforth "ZH"). This is applied here to shocks ranging from mildly to highly relativistic and shows that, as Γ_s rises from 2 to 50, the power-law index approaches the asymptotic value of $s = 4.17$ found by the eigenfunction method. This value is close to, but slightly harder than the result obtained previously for the case where scattering dominates both up and downstream.

In section 2 we formulate the equations describing particle transport, and present details of the first method of solution. Results of both methods, consisting of the power law index of accelerated particles and the angular dependence of their distribution function at the shock front, are presented and compared in section 3. In section 4 we discuss the physics underlying our assumptions and their range of applicability and speculate on the implications of the results for more realistic cases.

2 METHOD

2.1 Transport equation

In the presence of isotropic scattering in angle and gyration about a uniform field, the transport equation governing the phase-space density f of relativistic particles is given by eq (1) of Takamoto & Kirk (2015), (henceforth "TK"). Mixed coordinates are used in this equation, with Cartesian coordinates in configuration space measured in a frame in which the shock is at rest in the plane $x = 0$. The upstream plasma occupies the region $x > 0$, the downstream $x < 0$. Momentum space coordinates, on the other hand, are expressed in spherical polar coordinates, measured in the local (upstream or downstream) rest frame of the plasma. In this paper, we depart from the notation of TK and use the shock normal as the axis for these coordinates. Then, the momentum of an ultrarelativistic particle, in units of $c \times$ the rest mass, is $\vec{p} = (\gamma, \mu, \phi)$, with γ the Lorentz factor, $\arccos \mu$ the polar angle to the shock normal and ϕ the azimuthal angle about this axis. The direction of motion of the shock front in this reference frame is $\mu = 1$, and $\mu = 0$, $\phi = 0$, is the direction of the uniform magnetic field $\vec{B}$. Solutions are sought that are stationary as seen in the shock rest frame, and have no dependence on the spatial coordinates y and z. eq (12) of TK is then

$$\frac{2\Gamma^2 \eta c}{\omega_g} (\mu - \beta) \frac{\partial f}{\partial x} = \frac{\partial}{\partial \mu} \left(1 - \mu^2\right) \frac{\partial f}{\partial \mu} + \frac{1}{1 - \mu^2} \frac{\partial^2 f}{\partial \phi^2}$$
$$+ \frac{2\Gamma \eta \mu \cos \phi}{\sqrt{1 - \mu^2}} \frac{\partial f}{\partial \phi} - 2\Gamma \eta \sqrt{1 - \mu^2} \sin \phi \frac{\partial f}{\partial \mu}, \quad (1)$$

where $c\beta$ is the shock velocity measured in the local rest frame of the plasma, $\Gamma = \left(1 - \beta^2\right)^{-1/2}$ is the Lorentz factor of the shock front and we have assumed $\gamma \gg \Gamma$. The quantity η in this equation is the ratio of the gyro frequency of an accelerated particle in the uniform field, $\omega_g = |eB/\gamma mc|$, to Γ times the scattering frequency. Following Reville & Bell (2014), it can be written in terms of the magnetization parameter σ_{turb} associated with the strength δB of the magnetic fluctuations responsible for scattering, their characteristic length scale λ, the magnetization parameter σ_{reg} of the uniform, or *regular* upstream field and the ion plasma frequency ω_i:

$$\eta = \left(\frac{mc}{m_p \langle \gamma \rangle \omega_i \lambda}\right) \left(\frac{\sigma_{reg}^{1/2}}{\sigma_{turb}}\right) \left(\frac{\gamma}{\Gamma}\right), \quad (2)$$

where m and m_p are the rest masses of the accelerating particles and that of the species dominating the plasma inertia respectively, and $\langle \gamma \rangle m_p c^2$ is the mean energy per plasma particle. When $\eta \ll 1$, scattering dominates the transport process and deflections by the regular magnetic field are unimportant. We then refer to the particles as being unmagnetized. On the other hand, when $\eta \gg 1$, the particles are magnetized and follow essentially unscattered trajectories in the uniform, regular magnetic field. Equation (1) applies in both the upstream and the downstream regions, where the speeds of the relativistic shock are denoted by β_s and β_d, respectively, and the corresponding Lorentz factors are $\Gamma_s \gg 1$ and $\Gamma_d \sim 1$. Analogous notation, $\eta_{s,d}$, is used for the magnetization parameter.

2.2 Transport upstream

As is the case for particles accelerated at a parallel, ultrarelativistic shock front, we expect the stationary particle distribution in the upstream medium to be concentrated in a narrow cone of opening angle $\sim 1/\Gamma_s$ about the shock normal. Consequently, it is convenient

to replace μ by the *stretched* variable

$$\xi = (1 - \mu) / (1 - \beta_s) \quad (3)$$
$$\approx 2\Gamma_s^2 (1 - \mu)$$

(Kirk & Schneider 1989) which is zero for particles moving directly along the shock normal and unity for those moving parallel to the shock front. The phase-space density is now to be regarded as a function of x and the momentum space variables (γ, ξ, ϕ) that lie in the domain $\gamma > 1$, $0 \leq \xi < \infty$, $0 \leq \phi < 2\pi$ which we denote by A. Then, inserting the definition (3) into (1), expanding in powers of the small parameter $1/\Gamma_s$, and assuming the particles are unmagnetized:

$$\eta_s \ll 1, \quad (4)$$

the transport equation upstream becomes

$$\frac{\partial^2 f}{\partial \xi^2} + \frac{1}{\xi} \frac{\partial f}{\partial \xi} + \frac{1}{4\xi^2} \frac{\partial^2 f}{\partial \phi^2} - \left(\frac{1}{\xi} - 1\right) \frac{\partial f}{\partial \hat{x}} = 0, \quad (5)$$

where we have introduced the dimensionless coordinate $\hat{x} = x \left(4\Gamma_s^2 \omega_g\right) / (\eta c)$.

Equation (5) is separable, resulting in an exponential dependence of f on $\hat{x}$ and two eigenvalue problems, one for the ξ-dependence and one for the ϕ-dependence. Taken together with the boundary conditions (i) $f \to 0$ as $x \to \infty$, (ii) f bounded at $\xi = 0$ and ∞, (iii) f periodic in ϕ with period 2π and (iv) f invariant under a change of sign in the component of momentum parallel to the downstream magnetic field: $f(\gamma, \xi, \phi, x) = f(\gamma, \xi, \pi - \phi, x)$, each eigenvalue problem is self-adjoint. Therefore, the solution can be expanded in the two-dimensional eigenfunctions Q_i:

$$f(\gamma, \xi, \phi, x) = F(\gamma) \sum_{i=1}^{\infty} e^{\Lambda_i \hat{x}} a_i Q_i(\xi, \phi), \quad (6)$$

where the a_i are constants and the eigenfunctions are orthogonal over the weighting function $\xi - 1$:

$$\iint_{\vec{p} \in A} d\xi d\phi \, Q_i(\xi, \phi)(\xi - 1) Q_j(\xi, \phi) = 0, \quad i \neq j. \quad (7)$$

In Appendix A we give explicit expressions for the eigenvalues Λ_i and the eigenfunctions Q_i.

2.3 Transport downstream

Transport in the downstream plasma is potentially more complex, since the accelerated particles are not concentrated in a narrow beam when viewed from the frame in which the plasma is at rest. Here, we follow the arguments presented by Reville & Bell (2014), who conclude that deflection in the uniform magnetic field perpendicular to the shock normal dominates the transport process for particles with sufficiently large Lorentz factor, i. e.,

$$\eta_d \gg 1. \quad (8)$$

We concentrate on these high energy particles, because those of lower energy can be scattered in the turbulence generated at the shock front, and there is general agreement that the dominance of scattering on both sides of a relativistic shock results in a power law spectrum $f \propto \gamma^{-s}$ with index $s \approx 4.2$.

For $\eta = \eta_d \gg 1$ and $\Gamma = \Gamma_d \sim 1$, equation (1) reverts to Liouville's equation, albeit written in our unconventional mixed coordinate system. The distribution of particles that are too energetic to experience scattering downstream is, therefore, controlled by Liouville's theorem, which dictates that the phase-space density remains constant along particle trajectories. When viewed from a frame of reference
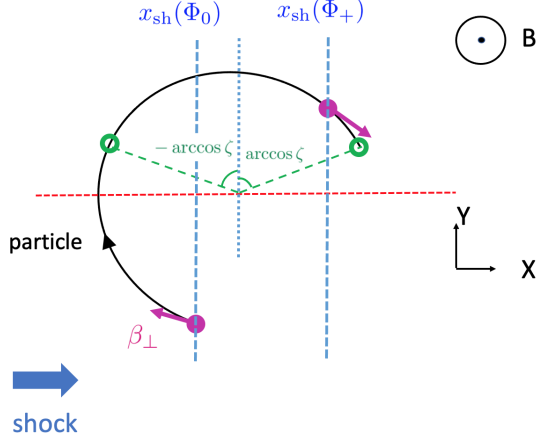
Figure 1. Sample trajectory for a positively charged particle with $\vec{p} \in R$ as seen in the downstream frame. The shock velocity and magnetic field are directed along the positive x and z axes respectively. The magnitude of the particle's velocity $\beta_\perp$ in the $x - y$ plane is a constant of motion, and its direction along the positive x axis when the phase Φ is an integer multiple of 2π. The filled magenta circles denote example positions where the particle enters and exits the downstream, at phases Φ_0 and Φ_+ respectively. To overtake the shock, the x-component of the particle velocity must exceed that of the shock, requiring $-\arccos\zeta < \Phi_+ < \arccos\zeta$, where $\zeta = \beta_d/\beta_\perp$. This range is delimited by the two green circles. For particles with $\vec{p} \in U$, we make the replacements $\Phi_0 \rightarrow \Phi_-$ and $\Phi_+ \rightarrow \Phi_0$. Further details are provided in Appendix B.

in which the downstream plasma is at rest these trajectories are simply helices along which the Lorentz factor γ remains constant.

At the shock front, $x = 0$, the domain of momentum space A can be divided into three non-overlapping sub-domains: (i) those trajectories crossing into downstream that subsequently return to the shock front, denoted by R (ii) those crossing into downstream that subsequently escape without re-encountering the shock, denoted by E, and (iii) those crossing into upstream, (i. e., all trajectories with $0 < \xi < 1$) denoted by U. Given the coordinates in momentum space $\vec{p} = (\gamma, \xi, \phi)$ of a trajectory in R, it is straightforward to compute the mapping $\mathcal{M} : R \rightarrow U$ that relates the point $\vec{p}$ on a particle trajectory to the point $\vec{p}_+ = (\gamma_+, \xi_+, \phi_+) = \mathcal{M}\vec{p}$ at which this trajectory returns to the shock front. In Figure 1, we provide a schematic sketch of a returning trajectory (for details see Appendix B). Then, Liouville's theorem requires the distribution at the shock front, $x = 0$ to satisfy

$$f(\vec{p}, 0) = f(\mathcal{M}\vec{p}, 0) \qquad \vec{p} \in R. \tag{9}$$

Conversely, given the coordinates of a trajectory that crosses the shock from downstream to upstream, one can simply invert this mapping to find the coordinates $\vec{p}_- = (\gamma_-, \xi_-, \phi_-) = \mathcal{M}^{-1}\vec{p}$ with which it previously entered the downstream region, which implies

$$f(\vec{p}, 0) = f(\mathcal{M}^{-1}\vec{p}, 0) \qquad \vec{p} \in U. \tag{10}$$

Liouville's theorem does not provide a constraint on the points $\vec{p} \in E$ on trajectories that escape from the shock into the downstream plasma, but it is convenient to define the mapping $\mathcal{M}$ to be unity when operating on these: $\mathcal{M}\vec{p} = \vec{p}$, $\vec{p} \in E$.

2.4 Approximation scheme

Since the problem, as formulated here, does not contain a characteristic scale for the particle Lorentz factor γ, we look for solutions that are a power law in this quantity, $F(\gamma) = \gamma^{-s}$. The index s is then

determined by matching the phase-space density across the shock front, i. e., by imposing the conditions (9) and (10) on the expression (6) for f in the upstream region, evaluated at the shock front $\hat{x} = 0$.

However, to find a numerical value for s, it is necessary to implement an approximation scheme. Here, we use a variant of the *Galerkin* method, similar to that used by Kirk & Schneider (1987), which essentially truncates the expansion (6) after the first i_{max} terms. Writing

$$f(\vec{p}, 0) = \gamma^{-s} \left[g_{i_{max}}(\xi, \phi) + \mathcal{R}_{i_{max}}(\xi, \phi) \right], \tag{11}$$

where

$$g_{i_{max}}(\xi, \phi) = \sum_{i=1}^{i_{max}} a_i Q_i(\xi, \phi) \tag{12}$$

is the desired approximation to the angular part of the distribution function at the shock front, we demand that the residual $\mathcal{R}_{i_{max}}$ be orthogonal to the first i_{max} eigenfunctions:

$$\iint_{\vec{p} \in A} \mathrm{d}\xi \mathrm{d}\phi Q_i (\xi - 1) \mathcal{R}_{i_{max}}(\xi, \phi) = 0 \ \text{ for } i = 1, \dots i_{max} \tag{13}$$

and, additionally, that the constraints (9) and (10) are satisfied not only by f, but also by its approximation, $\gamma^{-s} g_{i_{max}}$. This scheme can be motivated physically if the terms in the summation in eq (6) are ordered by the eigenvalue Λ_i, such that

$$\Lambda_i \geq \Lambda_{i+1}, \qquad i \geq 1. \tag{14}$$

Since $\Lambda_1 < 0$, the higher order terms in the expansion decay ever more rapidly with increasing distance from the shock in the upstream region. The particles described by these terms move almost in the plane of the shock, and, as a consequence, receive only a small boost in energy in a cycle of crossing and re-crossing. It is, therefore, to be expected that the index s is determined primarily by the first few terms in the summation.

Multiplying equation (11) by $\gamma^s Q_j$ and the weighting function, and integrating over $\vec{p} \in A$ leads to

$$\sum_{j=1}^{i_{max}} \left[D_{ij} - M_{ij}(s) \right] a_j = 0 \qquad i = 1, \dots i_{max}, \tag{15}$$

where the diagonal matrix D_{ij} results from substituting the expansion (6) into the left-hand side of (11):

$$D_{ij} = \iint_{\vec{p} \in A} \mathrm{d}\xi \mathrm{d}\phi \, Q_i(\xi, \phi)(\xi - 1) Q_j(\xi, \phi). \tag{16}$$

Similarly, the matrix $M_{ij}(s)$ is obtained from the right-hand side by applying the constraints (9) and (10) to the function $g_{i_{max}}$ and the constraint (13) to the function $\mathcal{R}_{i_{max}}$:

$$M_{ij}(s) = \gamma^s \iint_{\vec{p} \notin U} \mathrm{d}\xi \mathrm{d}\phi \, \gamma_+^{-s} Q_i(\xi, \phi)(\xi - 1) Q_j(\xi_+, \phi_+)$$
$$+ \gamma^s \iint_{\vec{p} \in U} \mathrm{d}\xi \mathrm{d}\phi \, \gamma_-^{-s} Q_i(\xi, \phi)(\xi - 1) Q_j(\xi_-, \phi_-). \tag{17}$$

Thus, eq (15) represents a system of homogeneous, linear algebraic equations for the a_j, which have a non-trivial solution only if

$$\mathrm{Det}\left[D_{ij} - M_{ij}(s)\right] = 0. \tag{18}$$

Given a guess for s, it is straightforward to evaluate these matrices by numerical quadrature. Then, a root-finder algorithm applied to equation (18) yields s and the coefficients a_i are found from the null-space of the corresponding matrix.
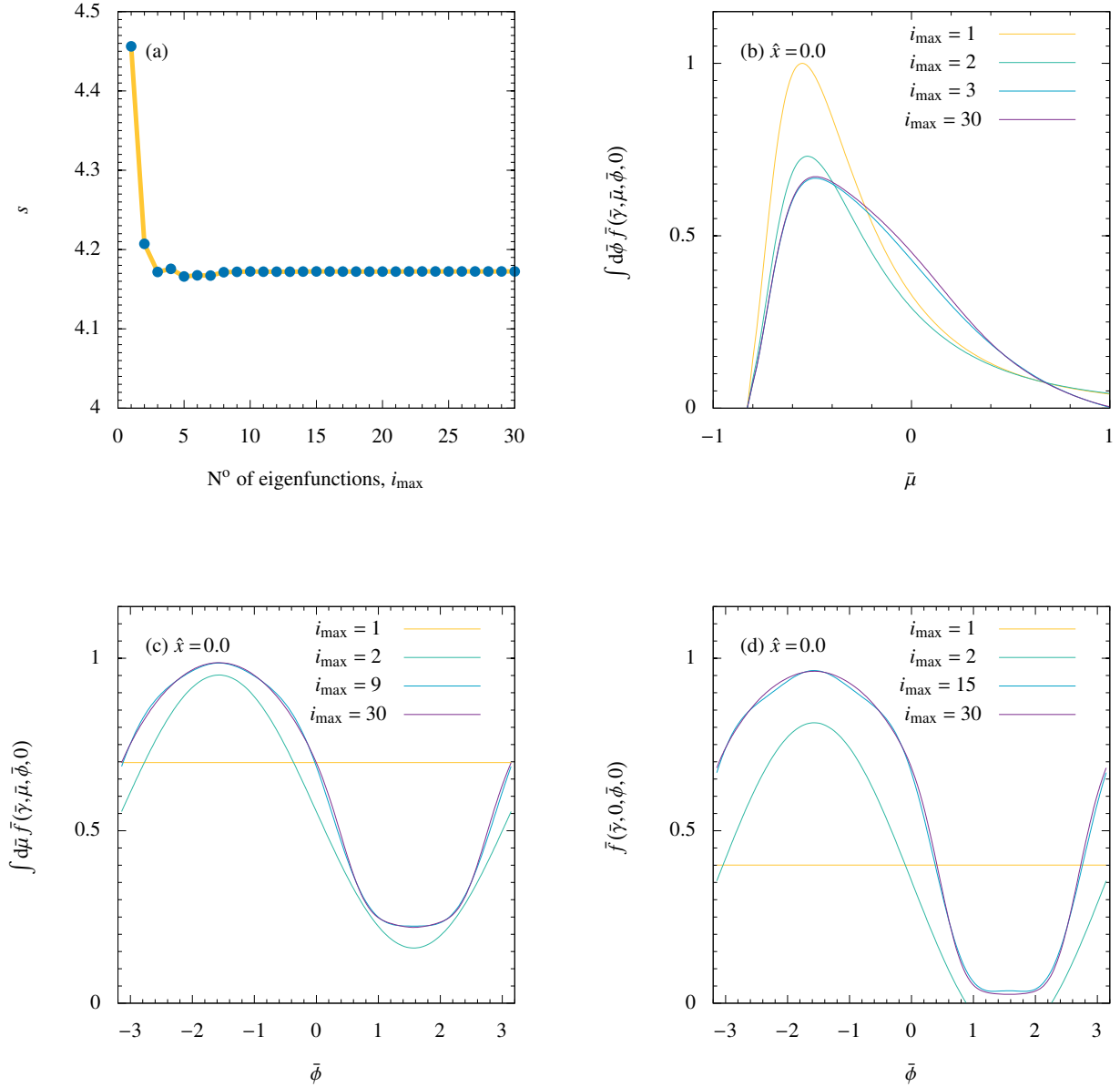
Figure 2. Convergence properties of the approximation scheme: (a) the power-law index s as a function of i_{max}, the number of eigenfunctions used in eq (12), (b) and (c) the phase space distribution $\bar{f}$ at the shock front ($\hat{x} = 0$) as seen in the frame in which the shock front is at rest, i. e., at constant particle Lorentz factor in this frame ($\bar{\gamma}$). $\bar{\mu}$ is the cosine of the angle between the particle momentum and the shock normal, $\bar{\phi}$ the azimuthal angle about this axis. Particles entering the upstream have $\bar{\mu} > 0$. (b) shows $\bar{f}$ averaged over phase, (c) $\bar{f}$ averaged over $\bar{\mu}$. (d) shows a slice of $\bar{f}$ for particles that graze the shock, $\bar{\mu} = 0$. Results are plotted for $i_{max} = 1, 2$ and the fully converged $i_{max} = 30$, as well as for an intermediate value that indicates the rapidity of convergence. In all cases the speed of the downstream plasma speed is $\beta_d = 1/3$. In (b), (c) and (d) only the relative values of the functions plotted is physically significant.

3 RESULTS

The usefulness of the approximation scheme described in 2.4 is confirmed by the rapid convergence as the number of eigenfunctions i_{max} is increased, as shown in fig 2. The converged value of s for an ultrarelativistic shock front in an ideal fluid, for which $\beta_d = 1/3$, is 4.17, close to, but slightly harder than the result found when particle transport is dominated by scattering both upstream and downstream. This value depends only on β_d, and is, in particular, independent of both the strength of the upstream scattering and the strength of the downstream magnetic field. As shown in panel (a) of Fig 2, convergence to this result requires only a few (~ 4) eigenfunctions. Because of the ordering of the eigenfunctions, equation (14), convergence of

the angular dependence of the phase space density is slowest at the shock front itself. Panels (b), (c) and (d) show this dependence as seen in the frame in which the shock is at rest, and the flow is directed along the shock normal. In this reference frame, the transformed spherical polar coordinates are denoted by $\bar{\gamma}, \bar{\mu}, \bar{\phi}$ where

$$\bar{\gamma} = \gamma \Gamma_s (1 - \beta_s \mu) \tag{19}$$

$$\bar{\mu} = (\mu - \beta_s) / (1 - \mu \beta_s) \tag{20}$$

$$\bar{\phi} = \phi \tag{21}$$

and, since the phase-space density, denoted in this frame by $\bar{f}$, is a Lorentz invariant quantity

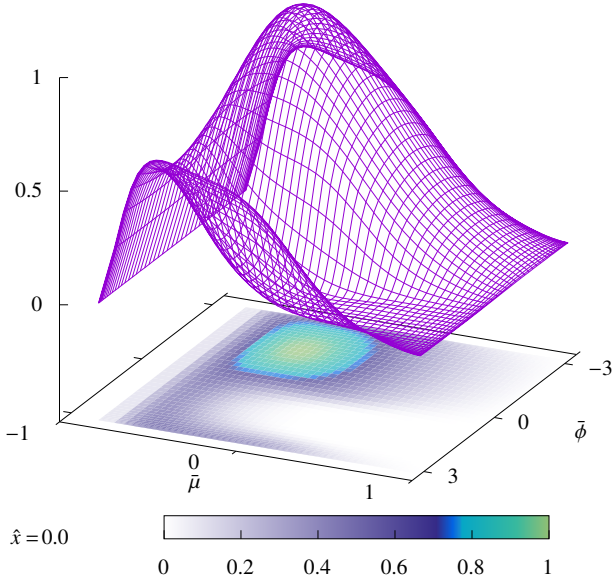$$\bar{f}(\bar{\gamma}, \bar{\mu}, \bar{\phi}, x) = f(\gamma, \mu, \phi, x) . \tag{22}$$

Figure 3. The full angular distribution of the phase space density $\bar{f}(\bar{\gamma}, \bar{\mu}, \bar{\phi})$ of accelerated particles at the shock front ($\hat{x} = 0$), as seen in the frame in which the shock front is at rest. The downstream magnetic field is in the direction $\bar{\mu} = 0$, $\bar{\phi} = 0$, particles crossing into the upstream region have $\bar{\mu} > 0$.

Note that although the average over either $\bar{\phi}$ or $\bar{\mu}$ of the distribution converges with only ~ 3 and ~ 9 eigenfunctions, respectively, the phase distribution of those particles that move precisely along the shock front converges much more slowly, needing ~ 15 eigenfunctions. This illustrates the fact that grazing particles have essentially no impact on the power law index.

The angular distribution at the shock front is, as expected, anisotropic. In addition to the anisotropy with respect to the shock normal, which is well-known from earlier studies of the scattering-dominated case and which arises because the relative velocity of the upstream and downstream plasmas is only slightly less than the particle velocity, a strong anisotropy in the azimuthal angle $\bar{\phi}$ is present because the downstream magnetic field imposes a drift along the shock front. This is clearly seen in the full 2-D angular distribution at the shock front, as shown Fig. 3. In terms of a right-handed system of coordinates with the magnetic field along the positive z-axis, the drift for a positively charged particle is in the positive y-direction ($\sin\bar{\phi} < 0$), i. e., in the direction opposite to that of the electric field seen in the shock rest frame. Thus, as seen in the rest frame of the shock, particles gain energy during an excursion upstream, but lose some on their downstream loop.

Monte-Carlo simulations, using the code described in ZH , provide an independent cross-check of these results, as well as extending them by lifting the restriction to the ultrarelativistic limit. In Fig 4, we compare the angular distributions found by both methods. Shock grazing particles are problematic in the Monte-Carlo approach when sampling the distribution precisely on the shock surface. Making the comparison a short distance upstream, here at the surface $\hat{x} = 0.1$, mitigates the problem. Results for the eigenfunction method are shown in the ultrarelativistic limit, since using a finite value of Γ_s would necessitate a numerical evaluation of the eigenfunctions. The Monte-Carlo simulations were performed with $\Gamma_s = 50$. Agreement is generally excellent, with small fluctuations visible only in the Monte-Carlo results for the full 2-D distribution.

The distribution of accelerated particles in energy for shock speeds ranging from mildly to highly relativistic is shown in Fig 5.

These are found using Monte-Carlo simulations that inject 10^6 particles into the upstream with $\gamma = 2\Gamma_s^2$, and a uniform angular distribution within a cone about the shock normal of opening angle $1/\Gamma_s$. The trajectories are then followed until they escape downstream, whilst registering the value of $\bar{\gamma}$ at each crossing of the shock. After several crossings, the distribution settles into a power law, that extends up to a point at which the statistical noise becomes significant. For simplicity, we choose in each case the jump conditions for a relativistic gas: $\beta_d\beta_s = 1/3$. The figure shows the distribution weighted by the factor $\bar{\gamma}^{4.17}$ in order to highlight the departure of the finite Γ_s results from the ultrarelativistic result found by the eigenfunction method. It can be seen that the power-law index s is within a few percent of its asymptotic value for $\Gamma_s > 5$.

4 DISCUSSION

Whether or not the mechanism of diffusive shock acceleration operates effectively at a perpendicular shock is a question that is still the subject of controversy, over four decades after the publication of the discovery papers, which implicitly addressed parallel shocks. In this context "effectively" means either that the acceleration rate is comparable to or faster than that at a parallel shock, or that the power-law index of the stationary phase-space distribution of accelerated particles is close to or harder than that produced at a parallel shock. The main result of this paper concerns the power-law index produced by highly relativistic, and, therefore, generically perpendicular shocks. Assuming that particles can be treated as unmagnetized when upstream of the shock (4), but as magnetized when downstream (8), we demonstrate quantitatively that these shocks are just as effective accelerators as the possibly less realistic parallel shocks addressed by previous analytical work. This result has major implications also for the expected acceleration rate, and the related maximum energy to which particles can be accelerated at a shock in a given physical situation, questions which are addressed in ZH .

The persistence of turbulence in the *downstream* medium at a level sufficient to demagnetize particles is generally perceived to be a major problem for the theory of diffusive shock acceleration at relativistic shocks (e. g., Bykov et al. 2012). Our assumption that turbulence is completely negligible downstream is specifically designed to address this point. It is, therefore, not restrictive, in the sense that diffusive acceleration can be expected to proceed as previously predicted if this assumption is not justified in a particular application.

On the other hand, the assumption that particles diffuse in angle when *upstream* of the shock is important. Unless a degree of randomness enters into the trajectories that return to the shock from upstream, diffusive acceleration will cease and particles will receive only a single, finite boost in energy before being swept away downstream (Begelman & Kirk 1990; Pelletier et al. 2009). We have adopted the simple prescription of isotropic diffusion to describe this randomness, since it renders the analytic approximations tractable; at least in the parallel shock case, this assumption does not appear to be crucial (Kirk et al. 2000). However, the validity of our approach does depend on the presence of turbulence of sufficient amplitude in the upstream medium. In the case of a weakly magnetized plasma $\sigma_{reg} < 10^{-3}$, such as might be encountered by the blast wave of a gamma-ray burst (GRB), a lower limit on the level of upstream turbulence is provided by shock-generated Weibel filaments, which, according to particle-in-cell simulations and analytical considerations, are amplified to $\sigma_{turb} \approx 0.1$. According to (2), this is already sufficient to demagnetize particles with $\gamma < 0.1 \times \Gamma_s \left(m_p/m \right) \sigma_{reg}^{-1/2}$,
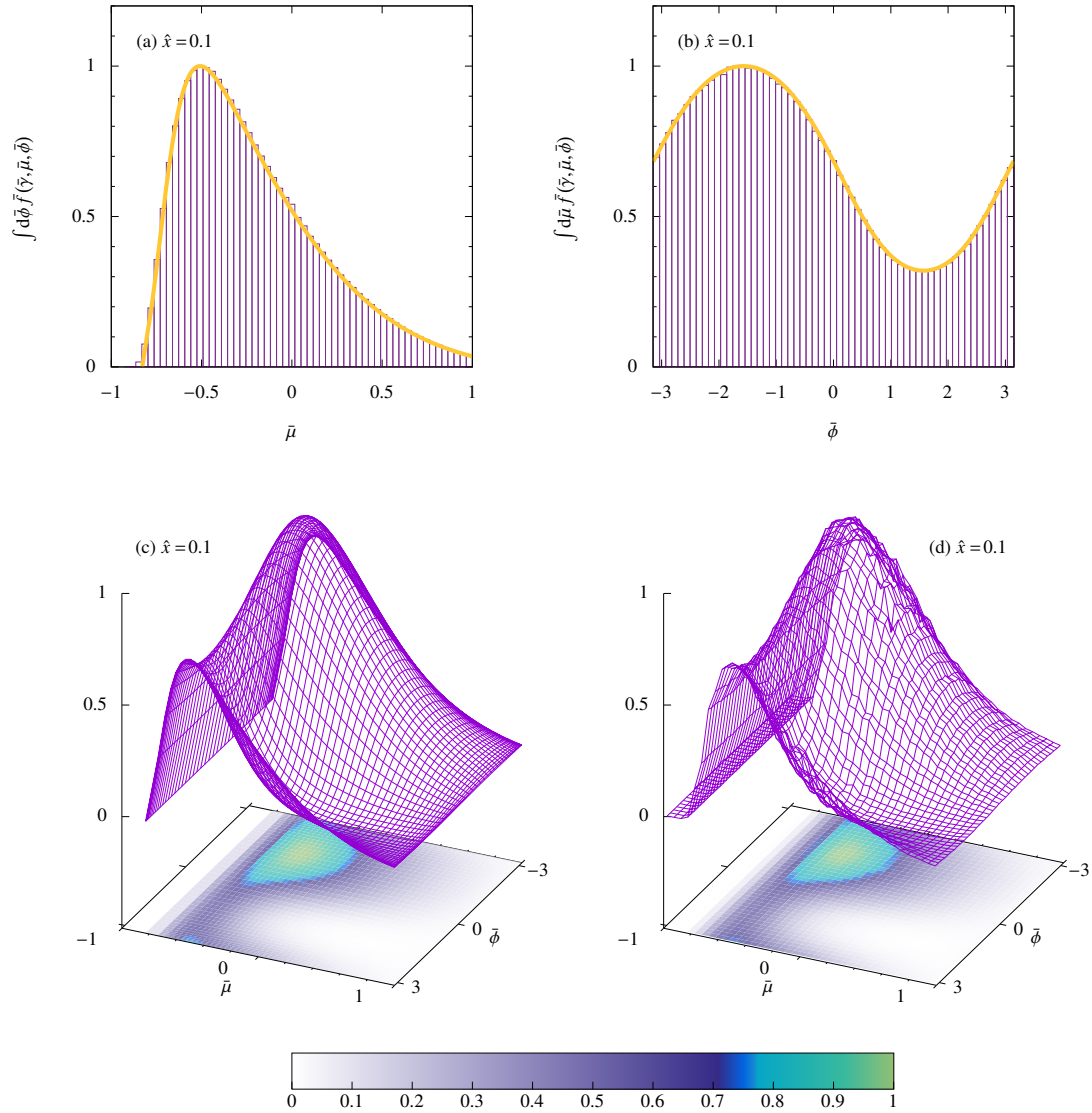
Figure 4. A comparison of the angular distributions just upstream of the shock front found by the eigenfunction method in the ultrarelativistic limit, and by Monte-Carlo simulation for $\Gamma_s = 50$. In (a) the distributions averaged over phase (about the shock normal), and, in (b), over the angle to the shock normal are compared. In each case the result for 30 eigenfunctions is shown as a yellow curve and that of the simulation as a purple histogram. In (c) and (d) the full distributions are shown for the eigenfunction and Monte Carlo methods, respectively.

and, therefore, enable diffusive acceleration even if the filaments are strongly damped downstream. However, this limit is unduly restrictive if turbulence exists in the upstream that is not directly excited by the processes that form the shock. In the case of a GRB, for example, the ionization, heating and pair-loading of the surrounding medium by the prompt emission (Beloborodov 2002; Grošelj et al. 2022) seems unlikely to leave behind a quiescent environment. Furthermore, turbulence is known to be present in the winds of the progenitors of some supernovae of the type Ibc (Wellons et al. 2012) that is associated with long duration GRBs. On the other hand, if the upstream medium is strongly magnetized, such as in the case of the termination shock of a pulsar wind, turbulence is embedded in the outflow by the pulsar and is thought to facilitate acceleration (Sironi & Spitkovsky 2011; Giacchè & Kirk 2017). Whereas previous discussions assumed this process to be confined to the equatorial region of the wind, where the regular field component vanishes, the results presented above suggest that it may persist to higher latitudes, with

interesting implications for modelling the emission from pulsar wind nebulae (Olmi et al. 2015).

In summary, if sufficient turbulence is present in the upstream medium, our results demonstrate that the perpendicular magnetic field in the plasma downstream of a relativistic shock front does not inhibit acceleration. Rather than being swept away without returning to the shock front, particles indeed return, and populate a power-law distribution whose index is insensitive to the nature of the dominant transport mechanism downstream.
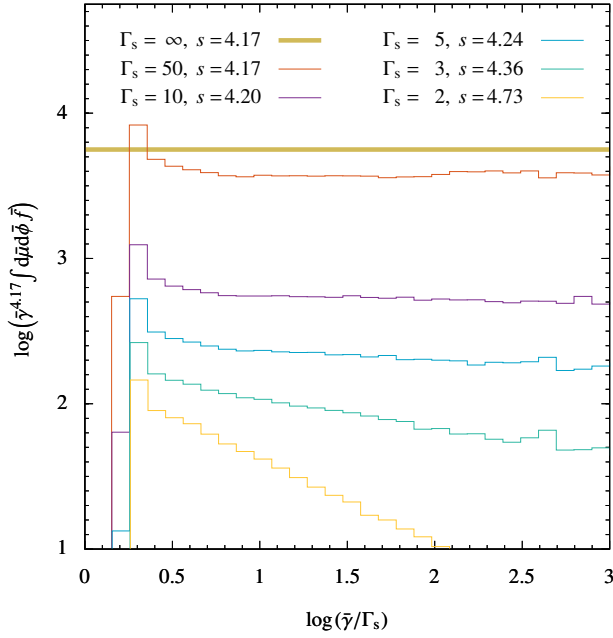
Figure 5. The angle-averaged distribution just upstream at $\hat{x} = 0.1$, as a function of the particle Lorentz factor $\bar{\gamma}$, measured in the rest frame of the shock. As the shock Lorentz factor Γ_s increases, the power-law section of the distribution converges towards the result found by the eigenfunction method in the ultrarelativistic limit, shown here as a horizontal line. For each Γ_s, the power-law index s, found from a least-squares fit to the data in the region $0.5 < \bar{\gamma}/\Gamma_s < 3$, is listed in the legend.

DATA AVAILABILITY

No data relevant to this paper are available.

REFERENCES

Achterberg A., Gallant Y. A., Kirk J. G., Guthmann A. W., 2001, MNRAS, 328, 393
Begelman M. C., Kirk J. G., 1990, ApJ, 353, 66
Bell A. R., 2014, Brazilian Journal of Physics, 44, 415
Beloborodov A. M., 2002, ApJ, 565, 808
Bykov A., Gehrels N., Krawczynski H., Lemoine M., Pelletier G., Pohl M., 2012, Space Sci. Rev., 173, 309
Chang P., Spitkovsky A., Arons J., 2008, ApJ, 674, 378
Giacchè S., Kirk J. G., 2017, ApJ, 835, 235
Grošelj D., Sironi L., Beloborodov A. M., 2022, ApJ, 933, 74
Huang Z.-Q., Kirk J. G., Giacinti G., Reville B., 2022, ApJ, 925, 182
Huang Z.-Q., Reville B., Kirk J. G., Giacinti G., 2023, to be submitted to MNRAS
Ince E. L., 1956, Ordinary Differential Equations. Dover Publications, Inc, New York
Keshet U., Katz B., Spitkovsky A., Waxman E., 2009, ApJ, 693, L127
Kirk J. G., Schneider P., 1987, ApJ, 315, 425
Kirk J. G., Schneider P., 1989, A&A, 225, 559
Kirk J. G., Guthmann A. W., Gallant Y. A., Achterberg A., 2000, ApJ, 542, 235
Lemoine M., 2015, Journal of Plasma Physics, 81, 455810101
Lemoine M., Pelletier G., 2010, MNRAS, 402, 321
Olmi B., Del Zanna L., Amato E., Bucciantini N., 2015, MNRAS, 449, 3149
Pelletier G., Lemoine M., Marcowith A., 2009, MNRAS, 393, 587
Plotnikov I., Grassi A., Grech M., 2018, MNRAS, 477, 5238
Reville B., Bell A. R., 2014, MNRAS, 439, 2050
Sironi L., Spitkovsky A., 2009, ApJ, 698, 1523
Sironi L., Spitkovsky A., 2011, ApJ, 741, 39
Sironi L., Spitkovsky A., Arons J., 2013, ApJ, 771, 54
Sironi L., Keshet U., Lemoine M., 2015, Space Sci. Rev., 191, 519
Takamoto M., Kirk J. G., 2015, ApJ, 809, 29
Vanthieghem A., Lemoine M., Plotnikov I., Grassi A., Grech M., Gremillet L., Pelletier G., 2020, Galaxies, 8, 33
Wellons S., Soderberg A. M., Chevalier R. A., 2012, ApJ, 752, 17

APPENDIX A: 2D EIGENFUNCTIONS

Inserting the expansion (6) into (5) and separating the variables according to

$$Q_i(\xi, \phi) = T_i(\xi) S_i(\phi) \tag{A1}$$

one obtains for the ϕ-dependent function

$$S_i'' = -j^2 S_i, \tag{A2}$$

where j is a constant, which, since S is periodic with period 2π, is an integer. Without loss of generality, we can choose $j \geq 0$ and identify two families of solutions that satisfy the additional symmetry $S_i(\phi) = S_i(\pi - \phi)$:

$$S_i \propto \begin{cases} \cos(j\phi) & j \text{ even or zero} \\ \sin(j\phi) & j \text{ odd}. \end{cases} \tag{A3}$$

The equation determining the ξ-dependent eigenfunction is

$$\left(\xi T_i'\right)' - \left[\frac{j^2}{4\xi} + \Lambda_i(1-\xi)\right] T_i = 0. \tag{A4}$$

Following Kirk & Schneider (1989, appendix A) (see also Ince (1956, section 7.31)), one looks for a solution of the form

$$T_i = e^{\lambda\xi} \xi^\alpha \sum_{n=0}^{\infty} c_n \xi^n. \tag{A5}$$

Inserting this into eq (A4), shows that the choice $\lambda = -\sqrt{-\Lambda_i}$ is convenient, since it removes the highest power of ξ in the term proportional to T_i, leading to a two-term recurrence relation for the c_n. The indicial equation is $\alpha^2 = j^2/4$, so that there are two possible solutions

$$T_i^+ = e^{-\sqrt{-\Lambda_i}\xi} \sum_{n=0}^{\infty} \xi^n c_n^+ \qquad j \text{ even or zero}$$

$$T_i^- = e^{-\sqrt{-\Lambda_i}\xi} \sum_{n=0}^{\infty} \xi^{n+\frac{1}{2}} c_n^- \qquad j \text{ odd}. \tag{A6}$$

Inserting (A6) into (A4) and equating coefficients gives $j^2 c_0^+ = 0$ and $\left(j^2 - 1\right) c_0^- = 0$ and, for $n \geq 0$, the recurrence relations

$$c_{n+1}^+ = \left(\frac{4\sqrt{-\Lambda_i}\left(2n+1-\sqrt{-\Lambda_i}\right)}{(2n+2)^2 - j^2}\right) c_n^+$$

$$c_{n+1}^- = \left(\frac{4\sqrt{-\Lambda_i}\left(2n+2-\sqrt{-\Lambda_i}\right)}{(2n+3)^2 - j^2}\right) c_n^-. \tag{A7}$$

Since $c_{n+1}^\pm / c_n^\pm \to 2\sqrt{-\Lambda_i}/n$, as $n \to \infty$ it follows that $T_i^\pm \to e^{\sqrt{-\Lambda_i}\xi}$ as $\xi \to \infty$, unless the relevant series truncates at finite n. Therefore, the eigenvalues satisfying the boundary conditions of boundedness at $\xi = 0, \infty$ are found by requiring truncation for, say, $n > k \geq 0$. Then,

$$\Lambda_i = \begin{cases} -(2k+1)^2 & j \text{ even or zero}, 0 \leq j \leq 2k \\ -4(k+1)^2 & j \text{ odd}, 1 \leq j \leq 2k+1, \end{cases} \tag{A8}$$

Table A1. 2D-eigenfunctions: i uniquely identifies the eigenfunction Q_i, j defines its ϕ-dependence according to eq (A3), k is the largest integer such that $c_k \neq 0$ in eq (A6), Λ_i is the eigenvalue determining the x-dependence associated with this eigenfunction in eq (6). The (arbitrary) normalisation of the Q_i is $c_n = 1$, where $n = j/2$ (j even or zero), or $n = (j-1)/2$ (j odd) is the smallest integer for which $c_n \neq 0$.

i	j	k	Λ_i	Q_i
1	0	0	-1	$e^{-\xi}$
2	1	0	-4	$e^{-2\xi}\sqrt{\xi}\sin(\phi)$
3	0	1	-9	$e^{-3\xi}(1-6\xi)$
4	2	1	-9	$e^{-3\xi}\xi\cos(2\phi)$
5	1	1	-16	$e^{-4\xi}\sqrt{\xi}(1-4\xi)\sin\phi$
6	3	1	-16	$e^{-4\xi}\xi^{3/2}\sin(3\phi)$

where k is a positive integer or zero. Thus, each index i corresponds to a pair of indices k and j. The eigenvalues Λ_i depend on k and only the parity of j. The corresponding eigenfunctions can be evaluated using the recurrence relations (A7). The first few are listed in Table A1.

APPENDIX B: MAPPING

For an ultrarelativistic particle ($\gamma \gg \Gamma_s$), membership of the three subdomains of momentum space at the shock front — upstream (U), returning (R) and escaping (E) — of the particle phase space (A) is determined solely by the direction of motion, labelled by the stretched variable ξ, defined in (3), and the azimuthal phase (with respect to the shock normal) ϕ. Membership of U requires only $\xi < 1$, but the requirements for R and E are more complicated. First, define the auxiliary parameter ζ to be the ratio of the shock speed $c\beta_d$ to the component $c\beta_\perp$ of the particle speed that is perpendicular to the magnetic field, both seen from the frame in which the downstream plasma is at rest. The computation of ζ from (ξ, ϕ) involves a Lorentz boost from the rest frame of the upstream plasma to that of the downstream plasma, followed by a change of axis of the polar coordinates from the shock normal to the magnetic field. To lowest order in $1/\Gamma_s$ one finds:

$$\zeta = \frac{\beta_d[(1+\beta_d)+(1-\beta_d)\xi]}{\sqrt{[(1+\beta_d)+(1-\beta_d)\xi]^2 - 4\xi(1-\beta_d^2)\cos^2\phi}} \geq \beta_d. \tag{B1}$$

This quantity remains constant during the particle's residence downstream. Clearly, $\zeta > 1$ implies that the particle cannot recross the shock front ($\vec{p} \in E$) and the mapping $\mathcal{M}$ is unity:

$$\mathcal{M}\vec{p} = \vec{p_+}, \; \vec{p} \in E:$$
$$\gamma_+ = \gamma \qquad \xi_+ = \xi \qquad \phi_+ = \phi. \tag{B2}$$

However, although $\zeta > 1$ is sufficient for $\vec{p} \in E$, it is not a necessary condition. The distance d, in units of the particle's gyroradius, between the shock and a point on the trajectory depends on ζ, the particle's phase Φ (measured about the downstream magnetic field, such that it is an increasing function of time for a positively charged

particle) and the phase Φ_0 at which the trajectory intersects the shock front:

$$d(\zeta, \Phi, \Phi_0) = \zeta(\Phi - \Phi_0) - (\sin\Phi - \sin\Phi_0). \tag{B3}$$

From the Lorentz boost and coordinate transformation, one finds, to lowest order in $1/\Gamma_s$,

$$\Phi_0 = \text{atan2}\left[2\sin\phi\sqrt{(1-\beta_d^2)\xi}, (1+\beta_d)-(1-\beta_d)\xi\right] + 2n\pi, \tag{B4}$$

where, to simplify the discussion, the integer n is to be chosen such that $-2\pi + \arccos\zeta \leq \Phi_0 < \arccos\zeta$. For $\vec{p} \notin U$, the distance d grows initially, implying $-2\pi + \arccos\zeta < \Phi_0 < -\arccos\zeta$, and subsequently goes through an alternating series of maxima and minima as the trajectory gyrates about the magnetic field. The first maximum is reached when $\Phi = -\arccos\zeta$ and the subsequent minimum when $\Phi = +\arccos\zeta$. Therefore, if $\zeta < 1$, a sufficient condition for the particle to escape is that $d > 0$ at this minimum, i. e.,

$$d(\zeta, \arccos\zeta, \Phi_0) > 0, \tag{B5}$$

in which case $\mathcal{M}$ is again the unit mapping (B2). If, on the other hand, $d < 0$ at this point, then $\vec{p} \in R$, and the phase Φ_+, with which the trajectory returns to the shock front, is given by the single solution of the equation

$$d(\zeta, \Phi_+, \Phi_0) = 0, \tag{B6}$$

with $-\arccos\zeta < \Phi_+ < \arccos\zeta$. Similarly, for $\vec{p} \in U$, which implies $-\arccos\zeta < \Phi_0 < \arccos\zeta$, the phase Φ_-, at which the trajectory previously entered the downstream region, is the single solution of the equation

$$d(\zeta, \Phi_0, \Phi_-) = 0, \tag{B7}$$

with $-2\pi + \arccos\zeta < \Phi_- < -\arccos\zeta$. Thus, the boundaries between the different subdomains for particles in R, E and U are uniquely defined in the $\Phi_0 - \zeta$ plane, as summarised in Figure B1.

To find $\mathcal{M}$, it remains to transform the coordinates and apply a Lorentz boost back to the upstream frame, which gives, to lowest order in $1/\Gamma_s$,

$$\mathcal{M}\vec{p} = \vec{p_+}, \; \vec{p} \in R \text{ and } \mathcal{M}^{-1}\vec{p} = \vec{p_-}, \; \vec{p} \in U:$$

$$\gamma_\pm = \gamma(\zeta + \beta_d\cos\Phi_\pm)\frac{(1-\beta_d)\xi + (1+\beta_d)}{2(1-\beta_d)\zeta}$$

$$\xi_\pm = \frac{(1+\beta_d)(\zeta - \beta_d\cos\Phi_\pm)}{(1-\beta_d)(\zeta + \beta_d\cos\Phi_\pm)}$$

$$\phi_\pm = \text{atan2}\left(\beta_d\sin\Phi_\pm, \sqrt{\zeta^2 - \beta_d^2}\right). \tag{B8}$$
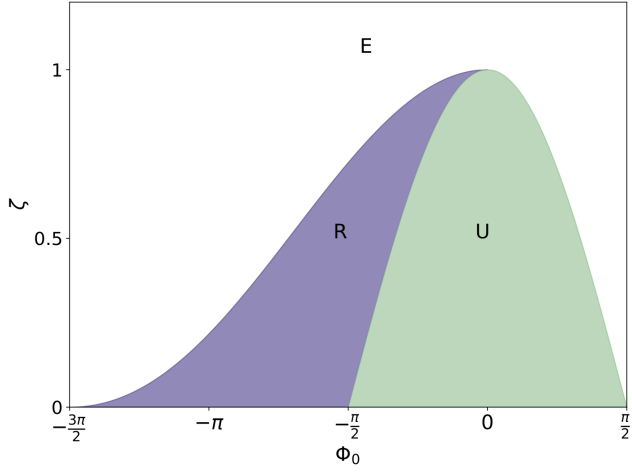
Figure B1. The three sub-domains of particle phase space at the shock front in the $\Phi_0 - \zeta$ plane: purple for $\vec{p} \in R$, green for $\vec{p} \in U$ and the remaining unshaded area for $\vec{p} \in E$. Note that $\zeta > \beta_d$.